MEDWAVE
PEER REVIEWED MEDICAL JOURNAL

RESEARCH

Mechanistic analysis of COVID-19 cases in Chile during the second half of 2020: an SIR model with dynamic transmission rate

Fernando Córdova Lepe[a], Ranghely Hernández Castañeda[b], Rodrigo Gutiérrez[c], Juan Pablo Gutiérrez Jara[d]*

[a]*Facultad de Ciencias Básicas, Universidad Metropolitana de Ciencias de la Educación, Santiago, Chile;* [b]*Doctorado en Modelamiento Matemático Aplicado, Universidad Católica del Maule, Talca, Chile;* [c]*Facultad de Ciencias Básicas, Universidad Católica del Maule, Talca, Chile;* [d]*Centro de Investigación de Estudios Avanzados del Maule, Universidad Católica del Maule, Talca, Chile*

ABSTRACT

INTRODUCTION This article analyzes the prolonged trough phase in the epidemic curve associated with COVID-19 dynamics in Chile during the period July-December 2020, characterized by a relatively stable daily record of 1 000-2500 cases.
METHODS Unlike traditional (β, γ)-SIR models, with constant parameters β and γ associated respectively with the transmission and removal rates in the infectious process, which predict unimodal behavior, we propose an approach based on Contagion Mechanics that incorporates a dynamic law for the transmission rate $\beta(\cdot)$.
RESULTS Using official data from the Department of Health Statistics and Information, we demonstrate how this approach quantitatively captures the observed stabilization, resulting from sustained adherence to non-pharmaceutical measures by the Chilean population. The model reveals that maintaining the infection rate below its intrinsic value required sustained collective effort, enabling controlled management of hospital demand during the pre-vaccination stage.
CONCLUSIONS Our results validate the usefulness of Contagion Mechanics in explaining complex epidemiological dynamics and offer new perspectives on the population response to prolonged health interventions.

KEYWORDS Epidemiology, Mathematics

INTRODUCTION

In general, the COVID-19 pandemic exhibited complex dynamics that challenged traditional mathematical modeling approaches across populations and observation levels [1,2]. In Chile, according to data from the Ministry of Health [3], following a first wave with a peak of 6938 daily cases reported in mid-June 2020, the epidemiological curve entered a phase of unusually prolonged stabilisation. As shown in Figure 1, from mid-July to the end of December 2020, daily confirmed cases remained predominantly between 1000 and 2500, forming an epidemiological 'trough'. From the perspective of mathematical modeling, this behaviour contrasts with the typical unimodal patterns predictable using traditional SIR or SEIR (Susceptible-Exposed-Infected-Removed) models with a constant transmission rate [5,6]. This intermediate period, prior to the second wave recorded in early 2021, constitutes a unique case study for analysing the cause-and-effect relationship between the non-pharmaceutical mitigation measures implemented in the pre-vaccine era and the maintenance of that trough.

Indeed, traditional mathematical models, based on the classic SIR compartmental model and assuming a constant transmission rate, are inherently incapable of reproducing sequences of peaks and troughs. This is because they tend to predict unimodal incidence curves with sharp peaks [7–9]. As Chowell et al. point out, "simple epidemic growth models assume constant transmission rates and homogeneous mixing, which generally results in unimodal incidence curves that do not capture the complex resurgence patterns observed in historical pandemics" [10]. It is widely accepted that temporal variability in the transmission rate, driven by behavioural changes, public

* **Corresponding author** jgutierrez@ucm.cl
Citation Córdova Lepe F, Hernández Castañeda R, Gutiérrez R, Gutiérrez Jara JP . Mechanistic analysis of COVID-19 cases in Chile during the second half of 2020: an SIR model with dynamic transmission rate. Medwave 2026;26(05):e3191
DOI 10.5867/medwave.2026.05.3191
Submitted Dec 4, 2025, **Accepted** Mar 19, 2026,
Published Jun 21, 2026
Postal address Avenida San Miguel 3605, Talca, Chile

MAIN MESSAGES

- Human behaviour plays a key role in the spread of disease, and in particular in the number of COVID-19 cases.
- This article presents a structurally simple mathematical model that provides a description reasonably consistent with data on the course of the COVID-19 pandemic in Chile.
- This work helps to rationalise decision-making by monitoring the dynamics without losing explanatory power.
- However, the model is not suitable for projections beyond the time period considered (July to December 2020).

health interventions and population adherence to these, is fundamental to explaining such dynamics [11]. In turn, Flaxman et al. [12] demonstrated that non-pharmaceutical interventions, particularly lockdowns, significantly reduced transmission by substantially altering the effective reproduction number.

Broadly speaking, there are two strategic modeling approaches to incorporate this variability:

1. Imposing an explicit, a priori functional form for the transmission rate (for example, a function that decreases over time) [13–16].
2. Incorporating a dynamic law governing its evolution as a function of the system's state variables [11,17].

Recently, the second approach has seen significant advances with the formulation of the mechanical theory of contagion [18–20]. An underlying objective of this article is to disseminate the language of the mechanical theory of contagion using a simple example represented by a basic model. Note that this theory provides a formal framework that allows the dynamics of the transmission rate to be derived from first principles, thereby avoiding ad hoc assumptions. These principles revolve around mechanisms of action and reaction associated with the loss and acquisition of intrinsic protective behaviours, linked to the implementation of pharmaceutical and non-pharmaceutical interventions [11,21,22]. Consequently, adherence to and compliance with these measures by the majority of the population influence the increase or decrease in the spread of the pathogen through social behaviour [23–26].

It is well documented that human behaviour is a key factor in fluctuations in the transmission rate [27–29]. The hypothesis put forward is that keeping the transmission rate below its natural or intrinsic level requires sustained behavioural effort on the part of the public. This led to a stabilisation which, in particular, allowed hospital demand to be kept generally below capacity, even taking into account capacity increases [30–33]. It should be noted that during this period, vaccines were not yet available [34].

In this context, our aim is to understand, from a general perspective, the behaviour of the infection rate in Chile during the period from July to December 2020, using the recent conceptual framework of the mechanical theory of contagion. We seek to quantify the collective effort required, in terms of reducing and stabilising the infection rate, to keep hospital demand at manageable levels. The results of the analysis not only validate the model's explanatory power but also offer a mechanistic perspective on the population's response to prolonged control measures in a critical scenario.

The article is structured into the following sections:

- **Methods**, where the theoretical framework of the β-SIR model is developed, formalising the incorporation of a

Figure 1. Daily number of COVID-19 cases reported in Chile by the WHO.

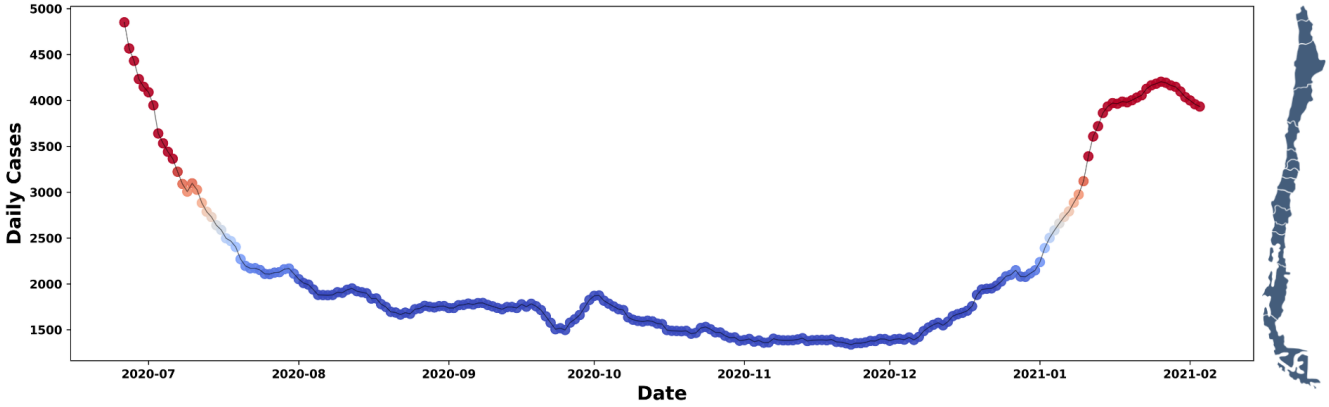

Period covered: 1 July 2020 to 31 January 2021.
The colours indicate the magnitude: red (≥ 3000); orange (2501 to 2999); and in blue (≤ 2500) we highlight a prolonged trough with a minimum of 1338 cases on 23 November 2020.
WHO: World Health Organisation.
Source: compiled by the authors based on WHO records [4].

variable transmission rate governed by mechanistic-behavioural principles.

- **Results**, in which a systematic numerical exploration is carried out to validate the model against data observed in Chile.
- **Discussions and conclusions**, where the findings are summarised and future research directions are outlined.

METHODS

We will consider a population affected by the spread of an infectious disease that follows the basic SIR compartmental epidemiological model. That is, each individual can be classified as susceptible (S), infectious (I) or recovered (R), and a unidirectional flow S →I →R is described by the system

$$S'(t) = -D(t), \quad I'(t) = D(t) - \gamma I(t) \quad y \quad R'(t) = \gamma I(t) \qquad (1)$$

Where $D(t)$ is the number of new cases, considering the time variable in days. Typically, the variable $D(\cdot)$ is expressed in accordance with the law of mass action, such that $D(t) = \beta(t)S(t)I(t)/N$, with $N = S + I + R$ the population size (constant), $\beta(\cdot)$ the transmission rate and γ - 1 the duration of the period of transmissibility.

Assuming that, in human populations, a threat to life triggers a defensive response in individuals (in a similar way to what occurs in ecological communities, where prey seek shelter in the presence or under direct threat of a predator [35]), it is possible to consider the existence of a population fraction f $(0 \le f \le 1)$ whether it adheres to non-pharmaceutical mitigation measures or disregards them (stops seeking shelter). All of this is based on an assessment of the size of the active group . This suggests that if is too high, then f $\mu_{max}(1 - f)$. Meaning, there exists a flow, less than or equal to μ_{max}, through which the non-refuigiated is added to f. Conversely, if I is comparatively low, then f $-\nu_{max} f$. This means that a maximum rate for the cessation of refugee status has been set.

Regarding μ_{max} and ν_{max}, which we shall refer to as the maximum protection factor and the maximum unprotected factor, respectively; note that both can be interpreted as upper bounds of their respective factors of the same name $\mu(I)$ and $\nu(I)$. These values reflect, over time, an assessment of the status of pathogen spread, for example through the number of active individuals $I(t)$ in the t-day. Thus, taking into account the natural growth pattern for the protection factor $\mu(I)$ and a decreasing trend for the vulnerability factor $\nu(I)$, we opted for technical simplicity and chose the following expressions:

$$\mu(I) = \mu_{max}\frac{I}{I + I_{u/2}} \quad and \quad \nu(I) = \nu_{max}\frac{I_{\nu/2}}{I + I_{\nu/2}} \qquad (2)$$

Let's observe in (2) that $\mu(\cdot)$ is strictly increasing, reaching half its maximum in $I_{\mu/2}$, while in $\nu(\cdot)$ is strictly decreasing, reaching half its maximum value at $I_{\nu/2}$.

Thus, the change in the refugee population, estimated based on the balance between daily arrivals and departures, is given by

$$f' = \mu(I)(1 - f) - \nu(I)f, \qquad \text{with} \qquad f_0 := f(0) \le 1. \qquad (3)$$

A key factor is understanding how this group of refugees affects the transmission rate $\beta(\cdot)$. To this end, the work by Melikechi O et al. [9] introduces the concept of an epi-band $V_{\delta,\tau}(P)$, defined as the spatiotemporal region surrounding an individual P, which makes it possible to determine whether contact has occurred when a person has remained at a maximum distance δ during a minimum τ time . This allows the transmission rate to be expressed as the product $\varkappa_{gen} \cdot \varrho$, where $\varkappa_{gen}$, known as the general contact rate, represents the average number of times per day that any given individual Q enters $V_{\delta,\tau}(P)$. The ϱ parameter indicates, in turn, the probability that, given contact between Q and P, being P infectious and Q infected.

If we consider the fraction f to represent the proportion of the population that is in isolation, it is to be expected that, under this assumption and given the lack of opportunities for contact, the overall number of contacts within the non-isolated population, $\varkappa^*_{gen}$, reduces in proportion f, adopting $(1 - f)\varkappa_{gen}$ the value. Therefore, assuming a constant transmission rate β_* in the absence of insulation, we have

$$\begin{aligned}\beta(t) = \varkappa_{gen}(t) \cdot \varrho = \left\{(1 - f(t))\,\varkappa^*_{gen}\right\} \cdot \varrho = \\ (1 - f(t))\left\{\varkappa^*_{gen}\varrho\right\} = (1 - f(t))\,\beta_*\end{aligned} \qquad (4)$$

Therefore, by deriving the identity in (4), we obtain β $= -f\beta_*$; and so, using (3), we have

$$\beta' = \{\mu(I)(1 - f) - \nu(I)f\}\beta_* = \nu(I)(\beta_* - \beta) - \mu(I)\beta \qquad (5)$$

This equation corresponds to the reaction–replenishment dynamic law governing the transmission rate that Córdova-Lepe and Vogt-Geisse [20] refer to $\mu(I)\beta(t)$. It represents the 'reaction rate', that is, the speed at which the population adopts protective behaviors. For its part, $\nu(I)(\beta_* - \beta(t))$ it corresponds to the 'restoration rate', the component that tends to bring the system back to the intrinsic rate β→ by analogy with the processes of isolation and exposure in the presence of an infectious agent.

Therefore, highlighting the dynamic nature of $\beta(\cdot)$ in the system (1)-(5), we shall denominate β-SIR to the system:

$$\begin{cases} \beta'(t) = \nu(I(t))(\beta_* - \beta(t)) - \mu(I(t))\beta(t), \\ S'(t) = -\beta(t)S(t)\dfrac{I(t)}{N}, \\ I'(t) = \beta(t)S(t)\dfrac{I(t)}{N} - \gamma I(t), \\ R'(t) = \gamma I(t). \end{cases} \quad (6)$$

With initial status $S(0), I(0)$ and $R(0)$ so that $S(0) + I(0) + R(0) = N$, and $\nu(\cdot)$ and $\mu(\cdot)$ are given by the functional structures presented in (2).

Introducing the concept of the 'intrinsic reproduction number', denoted by $R_0^* := \beta_*/\gamma$. Our study examines the case $R_0^* \;\>\; 1$. This represents, at least initially, an epidemiological spread. Therefore, in model (6), an initial transmission rate $0 \;\<\; \beta(0) \leq \beta_*$ is assumed. This reflects the existence of a level of public concern that causes the process to begin with a transmission rate that is lower than, or at most equal to, the intrinsic (natural) rate β_*.

Within the framework of contagion dynamics, introduced by Córdova-Lepe [18], the Second Law of Contagion concerns the balance between the strength of contagion $\boldsymbol{F}_I$ and forces of contact $\boldsymbol{F}_c$, represented in our work in $\boldsymbol{F}_I = (\beta I)'$ and $\boldsymbol{F}_c = I'\beta$, so that

$$\begin{aligned} \boldsymbol{F}_I - \boldsymbol{F}_c &= (\beta I)' - I'\beta \\ &= \beta' I + \beta I' - I'\beta \\ &= \beta' I \\ &= \underbrace{\nu(I)(\beta_* - \beta) I}_{\boldsymbol{F}^1_{ext}} - \underbrace{\mu(I)\beta I}_{\boldsymbol{F}^2_{ext}} \end{aligned}$$

where, denoted by $[\boldsymbol{t}]$ per unit of time (days) and by $[\boldsymbol{ind}]$ As for individuals, we see that two external forces are at work: one of protection $\boldsymbol{F}^1_{ext}$ and the other of desprotection $\boldsymbol{F}^2_{ext}$, defined by

$$\begin{aligned} &\boldsymbol{F}^1_{ext} = \nu(I)[\boldsymbol{t}]^{-1}(\beta_* - \beta(t))[\boldsymbol{t}]^{-1} I(t)[\boldsymbol{ind}] and \boldsymbol{F}^2_{ext} \\ &= \mu(I)[\boldsymbol{t}]^{-1}\beta(t)[\boldsymbol{t}]^{-1} I(t)[\boldsymbol{ind}]. \end{aligned}$$

Please note that we have highlighted the units $\left[\boldsymbol{ind}/\boldsymbol{t}^2\right]$ in line with the unit associated with the concepts of force introduced by Córdova-Lepe F [18].

Since our focus is on the transient behaviour of model (6) (a very specific initial period associated with 2020), an analysis of its long-term behaviour is not of interest to us. However, it should be noted that if $\beta(0) \leq \beta_*$, then $\beta(\cdot) \leq \beta_*$ always. Indeed, it is worth noting that, intuitively, mitigation measures and population responses can only reduce transmission below its natural level; they can never increase it above its intrinsic level. In fact, by defining the auxiliary function as $u(t) = \beta_* - \beta(t)$, we measure the deviation of the transmission rate from its intrinsic value. We calculate its derivative, and obtain: $u'(t) = \mu(I(t))\beta_* - [\nu(I(t)) + \mu(I(t))]u(t)$. Note that this is a non-homogeneous linear differential equation for $u(t)$. Let us consider the integral factor $\Phi(t) = exp(J(t)) \;\>\; 0$, with $J(t) = \int_{[0,t]}[\nu(I(s)) + \mu(I(s))]ds$, which is strictly positive for all $t \geq 0$. Multiplying both sides of the equation by $\Phi(t)$ and integrating this expression over 0 and t, the clearance is made:

$$u(t) = \left\{u(0) + \beta_* \int_0^t \Phi(s)\mu(I(s))ds\right\}/\Phi(t).$$

Therefore, we observe that $u(0) = \beta_* - \beta(0) \geq 0$, by hypothesis, we obtain $u(t) \geq 0$ for every $t \geq 0$. Equivalently, we have $\beta(t) \leq \beta_*$ for every $t \geq 0$.

This finding has significant epidemiological implications. The effective transmission rate never exceeds the intrinsic rate β_*. This confirms that social distancing and mitigation measures can only suppress transmission below its natural level; they can never increase it. This property ensures that the model adheres to a fundamental epidemiological threshold and provides a natural constraint on the system's dynamics.

RESULTS

Depending on different estimated values of the intrinsic reproduction number R_0^*, As reported by Navas & Vergara-Hermosilla [15], Tariq et al [36] and Canals et al [35], we analysed three epidemiological scenarios by fitting the model (1)–(5). To this end, the parameters were determined ν_{max}, μ_{max}, $I_{\nu/2}$and $I_{\mu/2}$, which define the dynamic law governing the reaction–recovery transmission rate (5). These parameters were estimated using the non-linear least squares method, implemented in Python via the function *scipy.optimize.leastsquares*. His routine is available via the following link: Google-Colaboratory

The initial conditions were derived from data reported by the Chilean Ministry of Health in its 10 July 2020 report [3]. In particular, the following were taken into account: $I(0)$= 26 390 active cases $R(0)$= 284 834 removed cases, that is, those who have recovered or died; together with a Chilean population of N = 19,660,000 individuals. Consequently, the number of susceptible individuals was calculated using the identity $S(0) = N - (I(0) + R(0))$, with a total of $S(0)$= 19 348 776 individuals.

Scenario 1

Taking into account an average incubation period of $\gamma^{-1} = 7$ days for an infectious individual, and an intrinsic transmission rate β_* calculated on the basis of the intrinsic basic reproduction number given by $\beta_* = R_0^*\gamma$, by $R_0^* = 1.8$ as reported by Navas and Vergara-Hermosilla [15], the following is obtained $\beta_* = 0.257$. The adjustment for new cases is illustrated in Figure 2.

The fit based on the non-linear least squares method yielded the following values $\mu_{max} = 1.55$ and $I_{\mu/2} = 10$, which means

Figure 2. Trend in new and estimated COVID-19 cases, scenario 1.

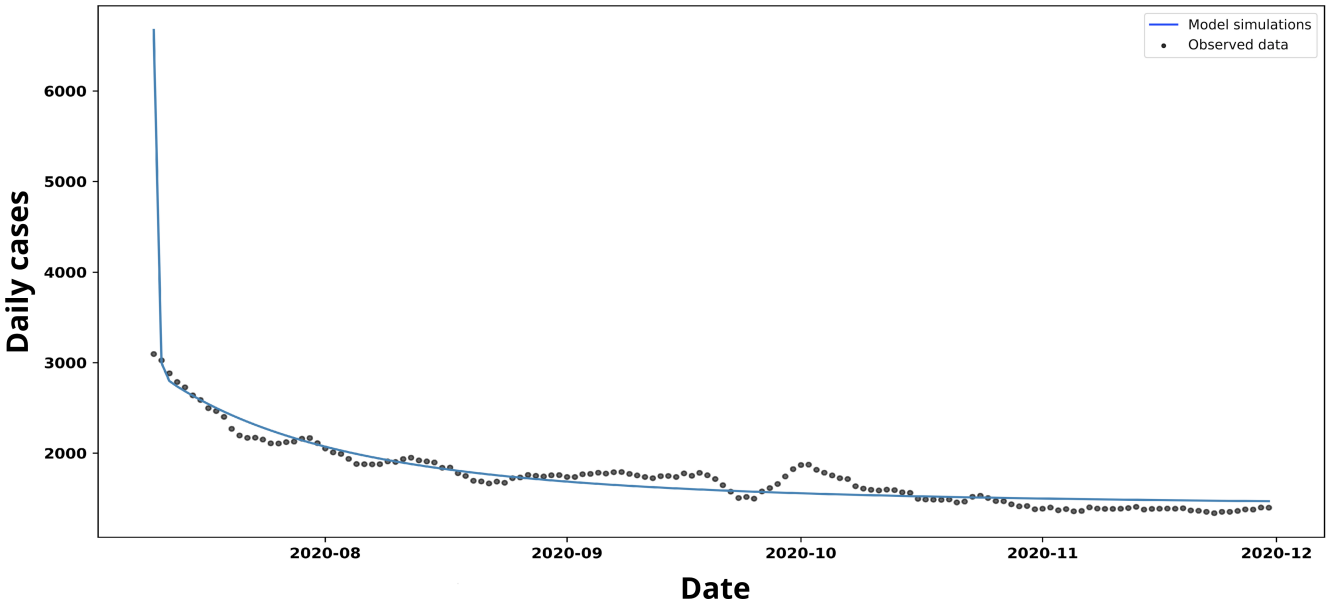

Data (black dots) and fit (blue line), based on model (6), showing the trend in COVID-19 cases in Chile from July to December 2020.
Source: Prepared by the authors based on the study's results.

that the protection factor meets $\mu(I) \approx \mu_{max}$. This is because the number of infectious people, $I(t)$, remains well above the threshold $I_{\mu/2}$ (Figure 3).

In Figure 3, $\beta(t)$shows a marked decline, influenced by the protective factor ($\mu(I) \approx \mu_{max}$) and low unprotected value ($\nu(I)$) at the start of the study. Subsequently, this transmission rate rises in line with the gradual increase in the vulnerability factor $\nu(I)$.

However, these adjusted values for protection and unprotection are difficult to identify in practice. As shown in the root mean square error (RMSE) curves in Figure 4, although both parameters can be estimated within the explored range, neither exhibits a clearly defined minimum. Rather than converging towards a clearly marked optimal value, the curves gradually flatten out and appear to settle at a local minimum.

This behaviour is consistent with what occurs during model fitting in this scenario: the parameters do not act independently. The epidemiological dynamics are non-linear and coupled, such that a change in any of the parameters alters the course of $S(t)$, $I(t)$ and $R(t)$. To compensate for these variations, the adjustment redistributes the values of the other parameters, generating different combinations of $[\nu_{max}, I_{\nu/2}, \mu_{max}, I_{\mu/2}]$ which produce simulated trajectories that are virtually indistinguishable. As a result of this internal compensation, the model can reproduce the data accurately across multiple parameter configurations. This makes it difficult to identify a single set of optimal values with precision.

The multiple configurations used for the simulations in Figure 4 were explored in a controlled manner by applying ±50% variations to the parameters ν_{max} and μ_{max} obtained using the least squares method. We observe that the changes in the shape of the simulated curves are relatively small, whilst the root mean square error shows much more pronounced variations. This means that, even when we make significant changes ν_{max} and μ_{max} and we re-optimise the remaining parameters, the overall dynamics of $S(t)$, $I(t)$and $R(t)$ remains virtually unchanged. This behaviour indicates that the model is not very sensitive in dynamic terms, but highly sensitive in terms of fit. This reinforces the idea that it allows multiple parameter combinations to generate similar trajectories.

SCENARIO 2

For the simulation of scenario two, shown in Figure 5, an initial transmission rate was implemented $\beta_0 = 0.37$, an intrinsic transmission rate $\beta^* = 0{,}81$ and a removal rate $\gamma = 0{,}426$ calculated by a relation $\gamma = \beta^*/R_0$, with a basic reproductive value $R_0 = 1.9$. These values were derived from the generalised growth model described by Tariq et al. in [36].

The curve of new cases shown in Figure 5 follows a trend very similar to that simulated using the parameters of Scenario 1. However, the model slightly overestimates the number of cases towards the end of the period, whilst fitting the data quite accurately from the first few weeks onwards.

The non-linear least squares fit shown in Figure 6 yielded the values for the protection and unprotection parameters $\mu_{max} = 4.62$, $I_{\mu/2} = 10$, $\nu_{max} = 19.5$ and $I_{\nu/2} = 1467$. A comparison between the model simulations under different scenarios (Figures 4 and 6) and the observed data shows that, even with small variations in transmission rates, the simulated curves maintain a generally stable shape, accurately capturing

Figure 3. Parameter tuning, scenario 1.

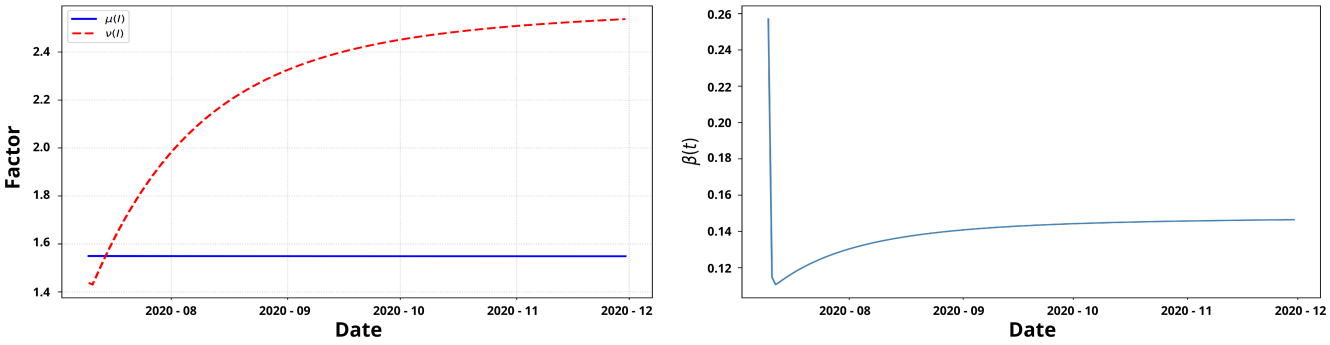

(a) Temporal evolution of factors μ and ν

(b) Temporal evolution of the transmission rate

In (a), simulation of the protection factors μ(I(t)).
In (b), corresponding behaviour of the dynamic transmission loop tβ(t).
Source: Prepared by the authors based on the study results.

Figure 4. Adjustment of protection and de-protection parameters, scenario 1.

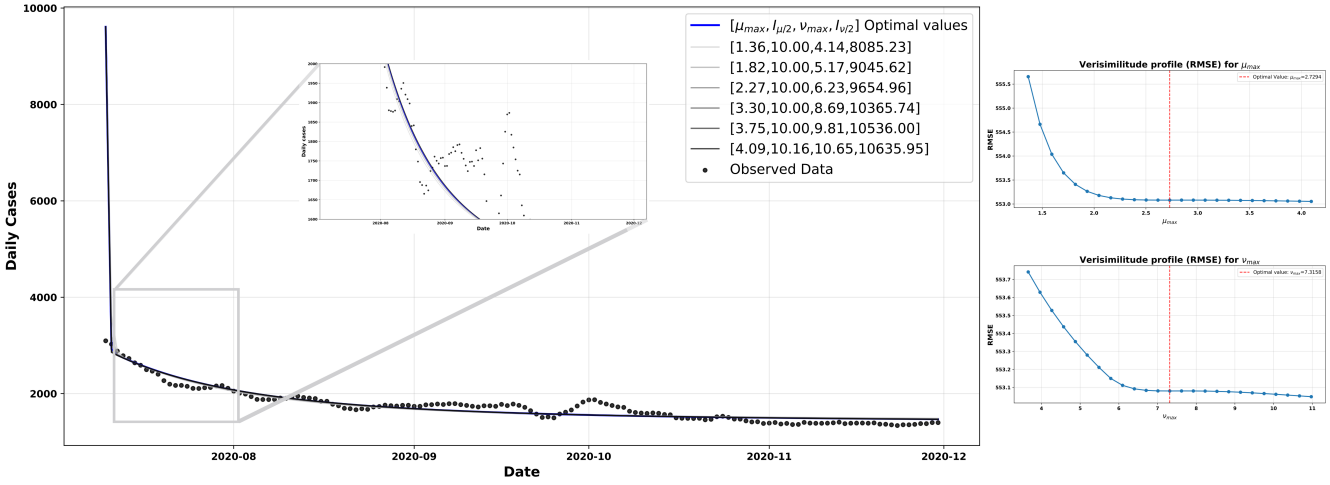

The left-hand side shows model simulations obtained by shifting the optimal values of the parameters μmax and Vmax' by 50%, compared with the observed data. On the right are the likelihood profiles based on the RMSE for μmax (top) and Vmax' (bottom), where the red vertical line indicates the estimated optimal value for each parameter.
RMSE: root mean square error.
Source: Prepared by the authors based on the study results.

the downward trend and plateau in the observed daily case numbers. This suggests that the model exhibits structural robustness, in the sense that its qualitative behaviour is not significantly affected by moderate changes in the parameters of the transmission mechanism. In other words, although the numerical values of β_0, β^* or even if the protective factors vary within a reasonable range, the simulated dynamics continue to consistently reproduce the observed trend in cases. This indicates that the system is stable in the face of moderate parametric perturbations, and that its qualitative conclusions do not depend critically on a single, precise set of parameters.

Scenario 3

In this scenario, we present the simulations based on the rates used and estimated by Canals et al [20]. In this study, the size of the Chilean population was taken as N = 19 000 000, and the period during which an individual remains infectious or dies was set at 14 days, then γ = 1/14 and a basic reproduction number in mid-June of less than 1, thus resulting in $\beta(0)$ = 0.0714. Furthermore, an average intrinsic basic reproduction number of $\beta_* = R_0\gamma$= 1.516, on the basis of which the intrinsic transmission rate was calculated β^*= 0.1082, under $\beta_* = R_0\gamma$ ratio.

The curve of new cases shown in Figure 7 exhibits a linear trend that differs significantly from the simulated curves in the previous scenarios. It can be seen that the β-SIR model (6) underestimates the initial number of new cases, but begins to align with the data by mid-August. This is likely due to the low initial transmission rate reported in mid-June [35], which may differ in July, the period covered by this study.

Figure 5. Trend in new and estimated COVID-19 cases, scenario 2.

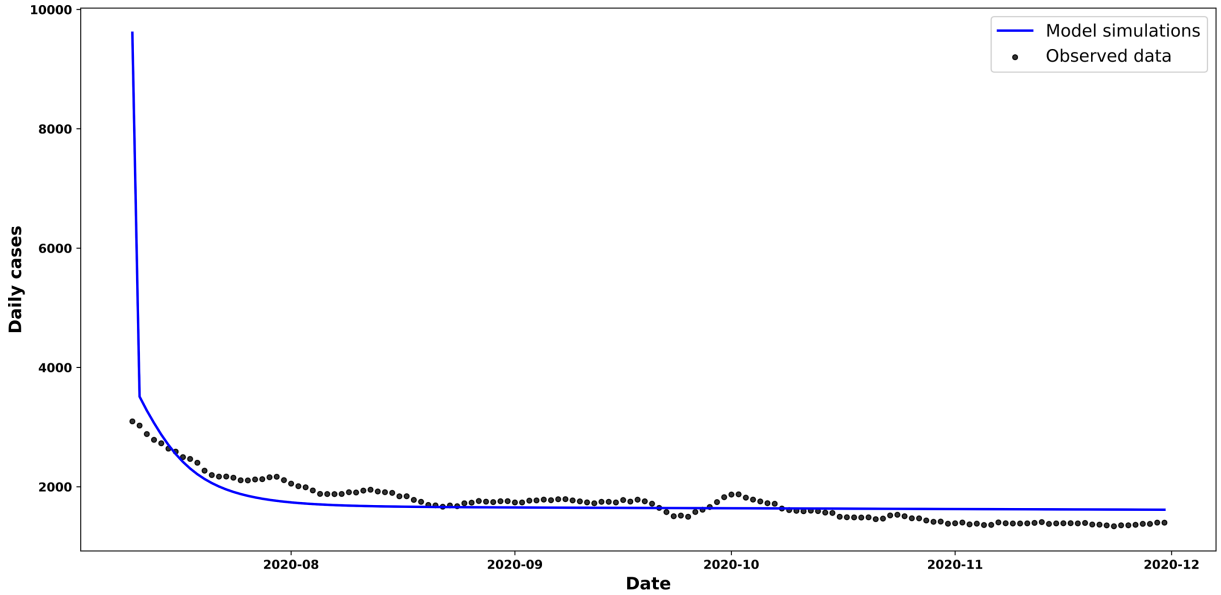

Comparative graph showing the trend in new COVID-19 cases in Chile and the trend in new cases estimated by our β-SIR model, as given by equation (6).
Source: prepared by the authors based on the study's results.

Figure 6. Adjustment of protection and de-protection parameters, scenario 2.

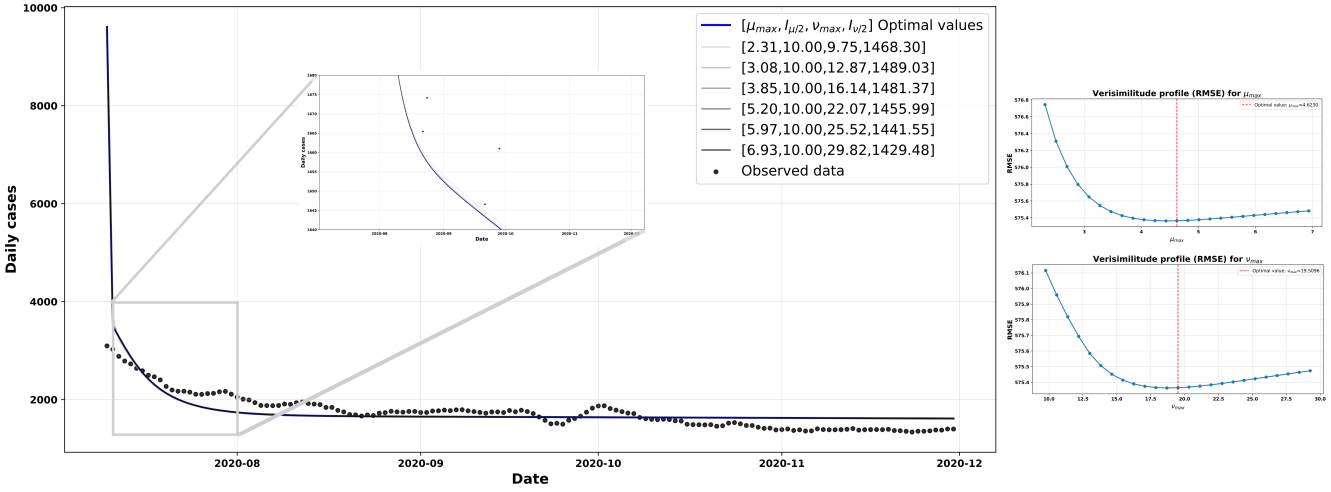

The left-hand side shows model simulations obtained by shifting the optimal values of the parameters μmax and Vmax' by 50%, compared with the observed data. On the right are the likelihood profiles based on the RMSE for μmax (top) and Vmax' (bottom), where the red vertical line indicates the estimated optimal value for each parameter.
RMSE: root mean square error.
Source: Prepared by the authors based on the study results.

The protection parameters set for this scenario were $\mu_{max} = 1.06 \times 10^{-4}$, $I_{\mu/2} = 10$. We obtain $\mu(I) \approx \mu_{max}$, given that the number of active cases remains very high compared with the threshold value $I/2$.

As for the adjusted vulnerability parameters, they were ν_{max} = 1 × 10^{-4} and $\beta_* = R_0\gamma$ 1 000 000. This indicates that the vulnerability factor $\nu(I) \approx \nu_{max}$, This occurs in this case because the threshold takes precedence $I_{\nu/2}$ on confirmed cases $I(t)$.

Consequently, the protective effect provided by $\mu(I)$ is essentially active at its maximum level, just like the unprotected factor $\nu(I)$. However, $\nu(I)$contributes less to the momentum because it is lower than $\mu(I)$. This combination explains the slight decline observed in the transmission rate $\beta(t)$ and active cases $I(t)$ in Figure 3.

The various configurations used for the simulations in Figure 8 were explored by applying ±50% variations to the parameters

Figure 7. Trend in new and estimated COVID-19 cases, scenario 3.
Comparative graph showing the trend in new COVID-19 cases in Chile and the trend in new cases estimated by our β-SIR model, as given by equation (6).

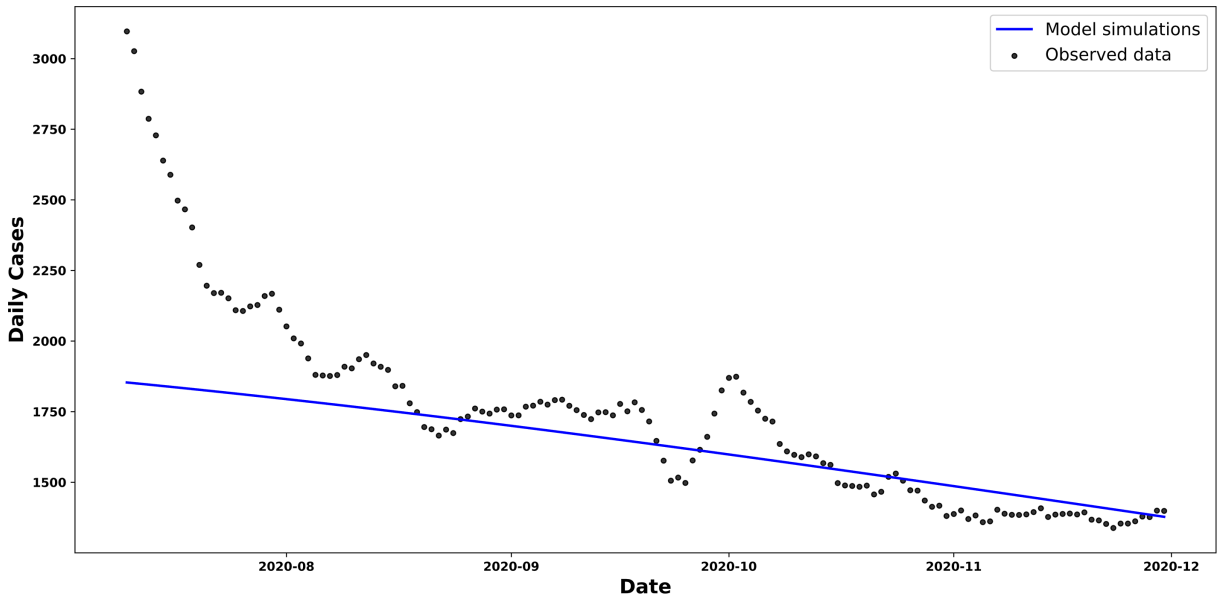

Source: prepared by the authors based on the study's results.

Figure 8. . Adjustment of protection and de-protection parameters, scenario 3.
The left-hand side shows model simulations obtained by shifting the optimal values of the parameters μmax and Vmax' by 50%, compared with the observed data. On the right are the likelihood profiles based on the RMSE for μmax (top) and Vmax' (bottom), where the red vertical line indicates the estimated optimal value for each parameter.

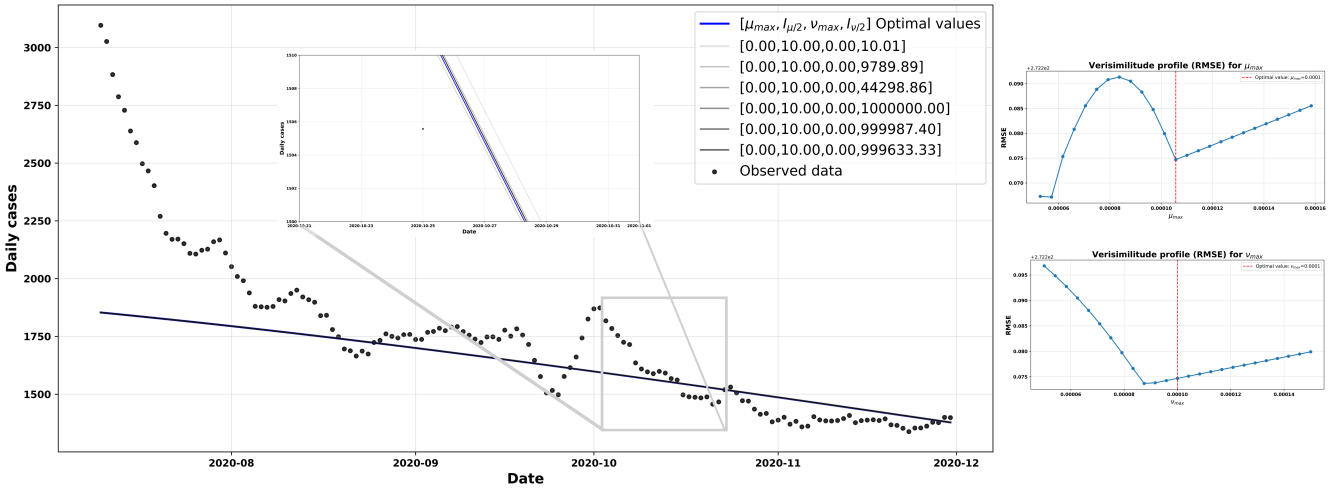

RMSE: root mean square error.
Source: Prepared by the authors of this study.

ν_{max} and μ_{max} obtained using the least squares method. We note that the changes in the shape of the simulated curves are again small, whilst the root mean square error = 272 is lower than in the previous scenarios.

Scenario 4

In this final scenario, we expanded our analysis by explicitly incorporating the effect of the non-pharmaceutical measures implemented in Chile on the model's dynamics. To do this, we used the composite stringency index. This indicator combines nine types of government interventions, including school and workplace closures, movement restrictions, and travel bans. This index ranges from 0 to 100, with higher values representing

Figure 9. Rigor index.
Variation in the rigor index with respect to μmax.

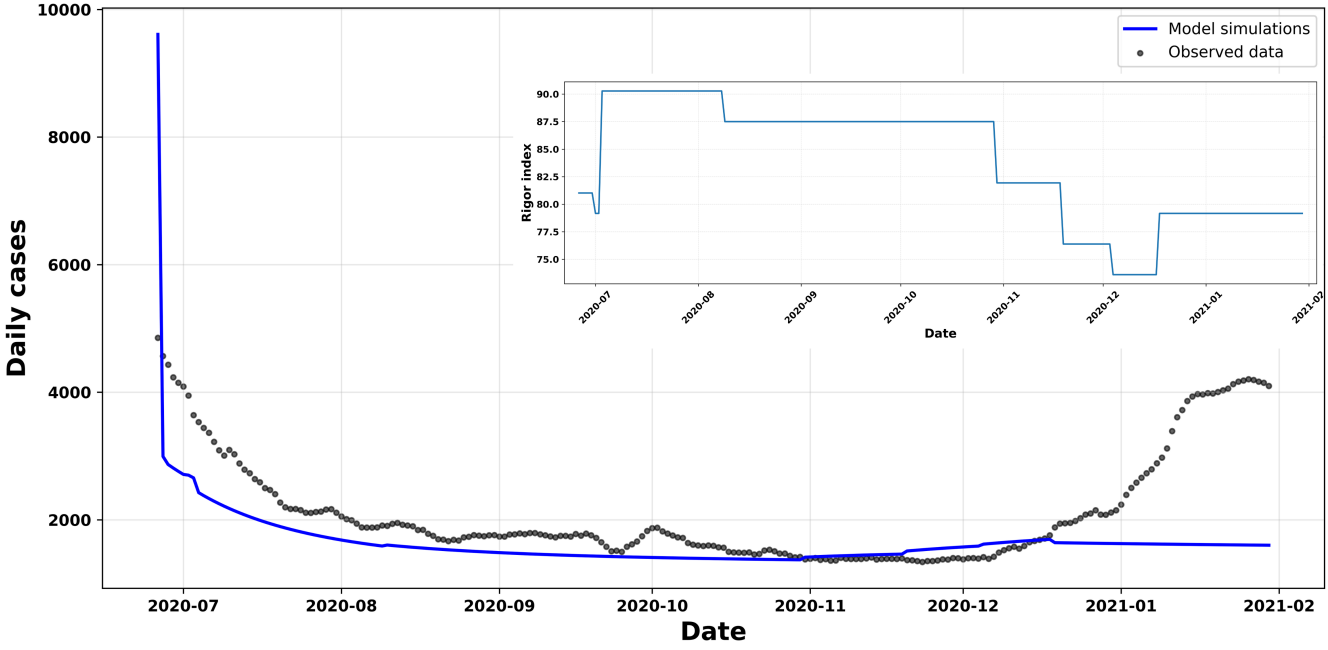

Source: compiled by the authors based on the study's results.

stricter policies, as reported by the World Health Organisation (WHO) [4].

The central idea was to allow the maximum protection parameter, μ_{max} , to respond directly to the temporal variation in this index. To this end, a simple proportional relationship was used:

$$\mu^*_{max} = \frac{\mu_{max}\ \text{stringencyindex}}{\text{averagestringencyindex}},$$

where the average stringency index was calculated over the period from 26 June 2020 to 30 January 2021, corresponding to the extended interval used in the simulation. Under this formulation, when the country adopts stricter measures, the protective effect incorporated into the model increases. Conversely, when measures are relaxed, this effect decreases. With this formulation, the initial conditions and parameters were selected μ_{max}, $I_{\mu/2}$, ν_{max}, $I_{\nu/2}$ optimised arbitrarily from scenario 1. Figure 9 shows the simulated behaviour compared with the observed data, reflecting the model's response to variations in the severity index over μ_{max}.

By incorporating the composite severity index into Figure 9, we observe that the parameters associated with the protection mechanism, in particular μ_{max}, vary in ways consistent with daily changes in the intensity of non-pharmaceutical measures. On days when measures are most stringent (for example, values close to 90), the model's simulation of new cases decreases, suggesting a greater ability of the population to enter a state of protection. Conversely, when the index decreases slightly (as occurs around 1 July), the maximum protection factor also decreases, reflecting lower protective pressure. Throughout the analysed period, this relationship remains stable and does not generate abrupt fluctuations in the parameters, indicating that the model responds consistently and robustly to moderate changes in stringency.

Taken together, these results show that the model is capable of adequately capturing the influence of public policies on the population's protective behaviour, whilst maintaining structural stability in its parameters throughout the adjustment.

Finally, we can observe in Table 1 that the model β-SIR As shown in (6), this provides a very good description of the trough in daily new COVID-19 cases during the period from July to December 2020. This suggests that the equations proposed for the protective and non-protective factors are appropriate.

Furthermore, the protective parameters applied to the transmission rate β—which were estimated using the non-linear least squares method within this model—enable us to determine, starting from the threshold of active cases ($I_{\mu/2}$), the extent to which non-pharmacological intervention policies and government-imposed mobility restrictions affect the Chilean population. Similarly, the μ_{max} estimate characterises the speed with which these mitigation measures are adopted.

The data suggest that these measures did not significantly impact the eradication of the disease. Chambon et al. [37] argue that the expected trajectory of the outbreak is influenced by the 'unengaged' or 'non-compliant' population in relation to non-pharmaceutical measures. Furthermore, they note that adherence to mitigation measures declines over time; and that

Table 1. Summary of parameters.

	Parameters							
	β_0	β_*	γ	μ_{max}	$I_{\mu/2}$	ν_{max}	$I_{\nu/2}$	RMSE
Scenario 1	0.2000	0.257	1/7	2.73	10	7.32	10049	553
Scenario 2	0.3700	0.810	0.426	4.62	10	19.50	1467	575
Scenario 3	0.0714	0.108	1/14	1.06×10^{-4}	10	1×10^{-3}	1 000 000	272
Scenario 4	0.2000	0.257	1/7	-	10	7.32	10049	837807

Abbreviations: RMSE, root mean square error.
Source: Prepared by the authors based on the study results.

factors such as pandemic fatigue, a perceived decrease in risk, and the normalisation of social contact limit the effectiveness of interventions.

The threshold value $I_{\nu/2}$ implemented in the transmission rate β, fitted using the non-linear least squares method under this model, allows us to determine the number of active cases at which the 'unengaged' or 'non-compliant' population begins to decline and accept the mitigation measures. Furthermore, the value of vmax allowed us to see the rate at which people adopt this type of disobedient behaviour.

Note that a common feature across all scenarios is the stabilisation of daily cases, a situation that persists as long as the external protective force $\boldsymbol{F}^2_{ext}$ and its inverse $\boldsymbol{F}^1_{ext}$ remain in effect. Therefore, as regards maintaining the model beyond December, this is not possible as complexities arise, such as variants, vaccination and various behavioural factors linked to the end-of-year festivities, the summer holidays or expectations regarding vaccination itself. These aspects mean that a model ceases to be a baseline model; it must incorporate additional compartments and account for varying intensity parameters. In this regard, to reproduce the January 2021 data (shown in orange or red in Figure 1), we vary the model parameters and obtain Figure 9.

DISCUSSION AND CONCLUSIONS

When faced with an epidemic curve, determining what constitutes a wave is not a settled matter, as there is no universal objective definition. This lack of consensus has direct consequences for detailed data analysis [38]. In this study, for the COVID-19 data in Chile during 2020, we have selected a period falling between the first two so-called waves. In a population of nearly twenty million people, the daily case curve shows relative stability which, at first glance (see Figure 1), forms a flat or trough-like section. We refer to what is commonly termed a trough, roughly bounded between early July (following a peak of 6,938 cases on 14 June [39]) and late December (prior to a new peak on 9 January 2021, with 4,956 cases). This period, associated with the dominant 'Delta' variant [40], shows a well-defined trough with a low of 1,352 cases on 22 November. This is of great interest for understanding the causes of this dynamic pattern of controlled or reduced transmission.

The literature suggests that these troughs may be due to a combination of factors, notably the depletion of susceptible individuals, seasonal changes, the effectiveness of control measures, and population behaviour. Ruling out the first two causes, we understand that, in the Chilean case, the observed stability is mainly associated with the implementation of health restrictions and a sufficiently alert population, willing to maintain, albeit to a decreasing extent, preventive behaviours. In this regard, the model with $\beta(\cdot)$ the dynamic described in Equation (6), and illustrated in Figure 2, is consistent with this interpretation. It is worth noting that similar periods of stability, in the form of troughs or plateaus, were observed in numerous countries, which reinforces the importance of the mitigation efforts undertaken by the respective health authorities [41].

It is possible to speculate that this trough began to disappear around January 2021, when figures rose again, probably due to behavioural factors associated with the end-of-year festivities, the start of the summer season and the announcement (on 16 December) of the arrival of 20,000 vaccine doses. This announcement materialised on the 24th of the same month, with the first person being vaccinated in the country [42].

The knowledge generated for decision-makers, most of whom belong to the medical community and the political sphere, is indispensable in the management of a high-risk infectious pandemic. For their part, mathematical models, given the phenomenon's complexity, constitute essential tools. Hence the need to strengthen educational efforts in this direction, in order to better understand the course of transmission processes [43].

The aim of this article has been to present a structurally simple mathematical model—for example, one with a small number of compartments—yet capable of providing a description that is reasonably consistent with the data. Undoubtedly, even simple models play a significant role in the monitoring of epidemics, as they help to rationalise decision-making by tracking the dynamics without losing explanatory power [44]. In particular, this approach allows for an interpretative reading grounded in the language of the mechanics of infection, which introduces a Newtonian analogy based on concepts of force. From this perspective, non-pharmaceutical mitigation measures can be understood as a reaction force exerted by the population, the counterpart to the intrinsic cultural and environmental pressure driving a return to a natural

state. However, the model is not viable for projections beyond the time interval considered. Indeed, after December 2020, it is no longer possible to assume that the system governing the dynamics remains a basic SIR model, as this assumption is unsustainable. This is because one must take into account the emergence of variants (non-homogeneous virulence and latency) and new structures arising from the multiplication of population compartments (for example, new infectious types), or the reduction in the susceptible population due to vaccination.

It should be noted that the usefulness or limitations of the mechanics of transmission—a theory which, in this paper, has been presented primarily as a descriptive and interpretative tool within a simplified empirical and theoretical context—depend on the modeler's ability to transpose, by analogy, the physics of classical mechanics of multi-component systems into the language of transmission forces offered by the theory. An example of this application is in more complex epidemiological scenarios, such as the forces acting on transmission rates differentiated according to some compartmentalisation criterion (such as infectious types). However, for a more direct and comprehensive understanding of the scope and limits of the mechanics of contagion, the reader is invited to delve into the seminal publications [11,19,20] and the dynamics of the novel theory [18].

Contributor roles FCL: conceptualization, methodology, formal analysis, writing (revisions and editing), supervision, research, data management, manuscript preparation (development of the original draft). RHC: methodology, formal analysis, writing (revisions and editing), research, data management. RG: methodology, formal analysis, writing (revisions and editing), research. JPGJ: methodology, writing (revisions and editing), research.

Competing interests The authors have completed the ICMJE conflict of interest disclosure form and declare that they received no funding for the preparation of this report; that they have had no financial relationships with organizations that might have an interest in the published article during the past three years; and that they have no other relationships or activities that might influence the published article. The forms may be requested by contacting the corresponding author or the journal's editorial office.

Ethics This study did not require review by an ethics committee because it was based on secondary sources.

Data sharing statement The authors state that they are willing to provide the research data upon request.

Language of submission Spanish.

Peer review and provenance Unsolicited. Peer-reviewed by three external reviewers using a double-blind review process.

REFERENCES

1. . Wang Z, Andrews MA, Wu Z-X, Wang L, Bauch CT.Coupled disease–behavior dynamics on complex networks: A review. Phys Life Rev. 2015;15: 1–29. https://doi.org/10.1016/j.plrev.2015.07.006
2. Cascante-Vega J, Torres-Florez S, Cordovez J, Santos-Vega M. How disease risk awareness modulates transmission: coupling infectious disease models with behavioural dynamics. R Soc Open Sci. 2022;9. https://doi.org/10.1098/rsos.210803
3. Ministerio de Salud de Chile. In: Datos epidemiológicos COVID-19[Internet]. 2020. https://deis.minsal.cl
4. World Health Organizaion. In: COVID-19 Cases, World[Internet]. https://data.who.int/dashboards/covid19/cases?n=c
5. Kuniya T. Structure of epidemic models: toward further applications in economics. Jpn Econ Rev (Oxf). 2021;72: 581–607. https://doi.org/10.1007/s42973-021-00094-8
6. Cuesta-Herrera L, Pastenes L, Córdova-Lepe F, Arencibia AD, Torres-Mantilla H, Gutiérrez-Jara JP. Analysis of SEIR-type models used at the beginning of COVID-19 pandemic reported in high-impact journals. Medwave. 2022;22: e2552–e2552. https://doi.org/10.5867/medwave.2022.08.2552
7. Turkyilmazoglu M. Explicit formulae for the peak time of an epidemic from the SIR model. Physica D. 2021;422. https://doi.org/10.1016/j.physd.2021.132902
8. Heng K, Althaus CL. The approximately universal shapes of epidemic curves in the Susceptible-Exposed-Infectious-Recovered (SEIR) model. Sci Rep. 2020;10. https://doi.org/10.1038/s41598-020-76563-8
9. Melikechi O, Young AL, Tang T, Bowman T, Dunson D, Johndrow J. Limits of epidemic prediction using SIR models. J Math Biol. 2022;85. https://doi.org/10.1007/s00285-022-01804-5
10. Chowell G, Sattenspiel L, Bansal S, Viboud C. Mathematical models to characterize early epidemic growth: A review. Phys Life Rev. 2016;18: 66–97. https://doi.org/10.1016/j.plrev.2016.07.005
11. Cabrera M, Córdova-Lepe F, Gutiérrez-Jara JP, Vogt-Geisse K. An SIR-type epidemiological model that integrates social distancing as a dynamic law based on point prevalence and socio-behavioral factors. Sci Rep. 2021;11. https://doi.org/10.1038/s41598-021-89492-x
12. Flaxman S, Mishra S, Gandy A, Unwin HJT, Mellan TA, Coupland H, et al. Estimating the effects of non-pharmaceutical interventions on COVID-19 in Europe. Nature New Biol. 2020;584: 257–261. https://doi.org/10.1038/s41586-020-2405-7
13. Cumsille P, Rojas-Díaz Ó, de Espanés PM, Verdugo-Hernández P. Forecasting COVID-19 Chile' second outbreak by a generalized SIR model with constant time delays and a fitted positivity rate. Math Comput Simul. 2022;193: 1–18. https://doi.org/10.1016/j.matcom.2021.09.016
14. Urena-Lopez LA. Time-dependent SI model for epidemiology and applications to Covid-19. Rev Mex Fís. 2021;67. https://doi.org/10.31349/RevMexFis.67.050706
15. Navas A, Vergara-Hermosilla G. Observaciones sobre la dinámica de la epidemia de Coronavirus y los casos no reportados: el caso de Chile.

16. Al-Salti N, Al-Musalhi F, ELmojtaba I, Gandhi V. SIR model with time-varying contact rate. Int J Biomath. 2021;14: 2150017. https://doi.org/10.1142/S1793524521500170
17. Spannaus A, Papamarkou T, Erwin S, Christian JB. Inferring the spread of COVID-19: the role of time-varying reporting rate in epidemiological modelling. Sci Rep. 2022;12. https://doi.org/10.1038/s41598-022-14979-0
18. Córdova-Lepe F. Mechanics of Contagion: A Newtonian Approach to Epidemiological Modeling. Epidemiology. 2025. https://doi.org/10.1101/2025.08.13.25333606
19. Córdova-Lepe F, Gutiérrez-Jara JP, Vogt-Geisse K. A Kinematic Approach to the Classical SIR Model. Axioms. 2024;13: 718. https://doi.org/10.3390/axioms13100718
20. Córdova-Lepe F, Vogt-Geisse K. Adding a reaction-restoration type transmission rate dynamic-law to the basic SEIR COVID-19 model. PLoS ONE. 2022;17. https://doi.org/10.1371/journal.pone.0269843
21. Reluga TC. Game theory of social distancing in response to an epidemic. PLoS Comput Biol. 2010;6. https://doi.org/10.1371/journal.pcbi.1000793
22. Howard J, Huang A, Li Z, Tufekci Z, Zdimal V, van der Westhuizen H-M, et al. An evidence review of face masks against COVID-19. Proc Natl Acad Sci USA. 2021;118. https://doi.org/10.1073/pnas.2014564118
23. Talic S, Shah S, Wild H, Gasevic D, Maharaj A, Ademi Z, et al. Effectiveness of public health measures in reducing the incidence of covid-19, SARS-CoV-2 transmission, and covid-19 mortality: systematic review and meta-analysis. BMJ. 2021;375. https://doi.org/10.1136/bmj-2021-068302
24. Chu DK, Akl EA, Duda S, Solo K, Yaacoub S, Schünemann HJ, et al. Physical distancing, face masks, and eye protection to prevent person-to-person transmission of SARS-CoV-2 and COVID-19: a systematic review and meta-analysis. The Lancet. 2020;395: 1973–1987. https://doi.org/10.1016/S0140-6736(20)31142-9
25. Nouvellet P, Bhatia S, Cori A, Ainslie KEC, Baguelin M, Bhatt S, et al. Reduction in mobility and COVID-19 transmission. Nat Commun. 2021;12. https://doi.org/10.1038/s41467-021-21358-2
26. . Córdova-Lepe F, Cabrera Hernández M, Gutiérrez-Jara JP.Modeling the epidemiological impact of a preventive behavioral group. Medwave. 2018;18: e7396–e7396. https://doi.org/10.5867/medwave.2018.08.7396
27. Funk S, Salathé M, Jansen VAA. Modelling the influence of human behaviour on the spread of infectious diseases: a review. J R Soc Interface. 2010;7: 1247–56. https://doi.org/10.1098/rsif.2010.0142
28. Ryan M, Brindal E, Roberts M, Hickson RI. A behaviour and disease transmission model: incorporating the Health Belief Model for human behaviour into a simple transmission model. J R Soc Interface. 2024;21. https://doi.org/10.1098/rsif.2024.0038
29. Arthur RF, Jones JH, Bonds MH, Ram Y, Feldman MW. Adaptive social contact rates induce complex dynamics during epidemics. PLoS Comput Biol. 2021;17. https://doi.org/10.1371/journal.pcbi.1008639
30. Liu Y, Morgenstern C, Kelly J, Lowe R, Jit M, CMMID COVID-19 Working Group. The impact of non-pharmaceutical interventions on SARS-CoV-2 transmission across 130 countries and territories. BMC Med. 2021;19. https://doi.org/10.1186/s12916-020-01872-8
31. Van Yperen J, Campillo-Funollet E, Inkpen R, Memon A, Madzvamuse A. A hospital demand and capacity intervention approach for COVID-19. PLoS ONE. 2023;18. https://doi.org/10.1371/journal.pone.0283350
32. Gutiérrez-Aguilar R, Córdova-Lepe F, Muñoz-Quezada MT, Gutiérrez-Jara JP. Model for a threshold of daily rate reduction of COVID-19 cases to avoid hospital collapse in Chile. Medwave. 2020;20. https://doi.org/10.5867/medwave.2020.03.7871
33. Rainisch G, Undurraga EA, Chowell G. A dynamic modeling tool for estimating healthcare demand from the COVID19 epidemic and evaluating population-wide interventions. Int J Infect Dis. 2020;96: 376–383. https://doi.org/10.1016/j.ijid.2020.05.043
34. In: Chile recibe primer cargamento de vacunas contra el COVID-19 a través de COVAX[Internet]. In: https://www.unicef.org/chile/comunicados-prensa/chile-recibe-primer-cargamento-de-vacunas-contra-el-covid-19-través-de-covax
35. Canals M, Cuadrado C, Canals A, Yohannessen K, Lefio LA, Bertoglia MP, et al. Epidemic trends, public health response and health system capacity: the Chilean experience in four months of the COVID-19 pandemic. Rev Panam Salud Publica. 2020;44. https://doi.org/10.26633/RPSP.2020.99
36. Tariq A, Undurraga EA, Laborde CC, Vogt-Geisse K, Luo R, Rothenberg R, et al. Transmission dynamics and control of COVID-19 in Chile, March-June, 2020. Epidemiology. 2020. https://doi.org/10.1101/2020.05.15.20103069
37. Chambon M, Dalege J, Borsboom D, Waldorp LJ, van der Maas HLJ, van Harreveld F. How compliance with behavioural measures during the initial phase of a pandemic develops over time: A longitudinal COVID-19 study. Br J Soc Psychol. 2023;62: 302–321. https://doi.org/10.1111/bjso.12572
38. Ayala A, Villalobos Dintrans P, Elorrieta F, Castillo C, Vargas C, Maddaleno M. Identification of COVID-19 Waves: Considerations for Research and Policy. Int J Environ Res Public Health. 2021;18. https://doi.org/10.3390/ijerph182111058
39. Canals M. In: Informe Covid-10[Internet]. 2022. https://facso.uchile.cl/dam/jcr:0951afd1-5ba2-4d10-b466-933325f53104/ACTUALIZACION%20COVID-19%202022%20AL%2020-03-2022.pdf
40. Barría-Sandoval C. Modelos de Series de Tiempo para Predecir el Número de Casos de Variantes Dominantes del SARS-COV-2 Durante las Olas Epidémicas en Chile. RP. 2022;50: 17–26. https://revistapolitecnica.epn.edu.ec/ojs2/index.php/revista_politecnica2/issue/view/53https://doi.org/10.33333/rp.vol50n3.02

41. Leiva V, Alcudia E, Montano J, Castro C. An Epidemiological Analysis for Assessing and Evaluating COVID-19 Based on Data Analytics in Latin American Countries. Biology (Basel). 2023;12. https://doi.org/10.3390/biology12060887
42. Red Salud SSMSO. In: TENS Zulema Riquelme del Hospital Sótero del Río fue la primera vacunada en Chile contra el COVID-19[Internet]. 25Dec2020. In: https://redsalud.ssmso.cl/tens-zulema-riquelme-del-hospital-sotero-del-rio-fue-la-primera-vacunada-contra-covid-19
43. González-Fuenzalida F, González-Cohens F. Epidemias en la actualidad: de cómo los modelos matemáticos y estadísticos permiten entenderlas, aún a profesionales "adversos" a ellos. Rev méd Chile. 2021;149: 422–432. https://doi.org/10.4067/s0034-98872021000300422
44. Canals M, Cuadrado C, Canals A. COVID-19 in Chile: The usefulness of simple epidemic models in practice. Medwave. 2021;21. https://doi.org/10.5867/medwave.2021.01.8119

Análisis mecanicista de los casos de COVID-19 en Chile durante el segundo semestre de 2020: un modelo SIR con tasa de transmisión dinámica

RESUMEN

INTRODUCCIÓN Este artículo analiza la prolongada fase valle en la curva epidémica asociada a la dinámica de COVID-19 en Chile durante el periodo de julio a diciembre de 2020, caracterizada por un registro relativamente estable entre 1000 y 2500 casos diarios.
MÉTODOS A diferencia de los modelos (β, γ)-SIR tradicionales, con parámetros constantes β y γ asociados respectivamente a la tasa de transmisión y de remoción en el proceso infectocontagioso, los cuales predicen comportamientos unimodales; proponemos un enfoque basado en la mecánica del contagio que incorpora una ley dinámica para la tasa de transmisión $\beta(\cdot)$.
RESULTADOS Utilizando datos oficiales del Departamento de Estadísticas e Información de Salud, demostramos cómo esta aproximación captura cuantitativamente la estabilización observada, resultado de la adherencia sostenida a medidas no farmacéuticas por parte de la población chilena. El modelo revela que mantener una tasa de contagio por debajo de su valor intrínseco requirió un esfuerzo colectivo constante. Ello permitió un manejo controlado de la demanda hospitalaria en la etapa prevacunal.
CONCLUSIONES Nuestros resultados validan la utilidad de la mecánica del contagio para explicar dinámicas epidemiológicas complejas. Además, ofrecen nuevas perspectivas sobre la respuesta poblacional frente a intervenciones sanitarias prolongadas.